EUROPHYSICS LETTERS 15 October 2006

Europhys. Lett., **76** (2), pp. 229–235 (2006)
DOI: 10.1209/epl/i2006-10267-5

Wave self-modulation in an acoustic resonator due to self-induced transparency

L. Fillinger[1], V. Zaitsev[2], V. Gusev[1] and B. Castagnède[1]

[1] *Université du Maine - Avenue Olivier Messiaen, 72085 Le Mans Cedex 09, France*
[2] *Institute of Applied Physics RAS - 46 Uljanova St., Nizhny Novgorod, Russia*

received 7 July 2006; accepted in final form 29 August 2006
published online 20 September 2006

PACS. 43.25.+y – Nonlinear acoustics.
PACS. 05.45.-a – Nonlinear dynamics and chaos.
PACS. 46.40.Ff – Resonance, damping, and dynamic stability.

Abstract. – Observations and interpretation of modulation instability (MI) in an acoustic resonator with a crack-like defect are presented. This MI is similar in appearance to the conventionally disscussed MI, which arises due to the interplay between the reactive nonlinearity and velocity dispersion. However, the observed MI is due to an essentially different, purely dissipative, mechanism that can be common for waves of different physical nature. The mechanism exhibits interesting peculiarities, for example, the MI threshold can only be reached when the excitation frequency does not coincide with the resonator eigenfrequencies.

Modulational instability (MI) is a nonlinear phenomenon manifesting itself in various areas of physics including laser optics and plasma physics, fluid dynamics, chemistry and biology, etc. and leading to spatial and/or temporal pattern formation and chaos [1–3]. MI is known to happen for elastic waves as well [4–7]. Omitting details specific for a particular wave origin, conventionally considered MI mechanisms can be roughly subdivided into three main groups.

The first most often discussed MI mechanism implies the interplay between odd-type nonlinearity and wave velocity dispersion [1,8]. At certain conditions (proper signs of nonlinearity and dispersion) these factors result in instability of the uniform envelope and in appearance of slow (at scale of the carrier frequency) modulation up to formation of envelope solitons. This mechanism can be formalized based on Schrödinger-type dissipation-free equations with cubic reactive nonlinearity [1, 5, 6, 8]. Similar MI effects may also arise due to odd-type piecewise quadratic hysteretic nonlinearity (combining reactive and dissipative parts) [9] or due to non-instantaneous (relaxing or integrating) nonlinearity [10].

Another group of MI phenomena is typical of laser physics, where media may be active (with negative dissipation), so that the interplay between the activity-induced instability and effects of either depletion of the pumping or influence of saturating absorption cause modulation of the resultant radiation (up to strongly pulsed regimes) [1, 2].

An essentially different group of MI phenomena (discussed mostly for acoustics, but also applicable to other situations) imply more indirect mechanisms based on the parametric decay instability of the primarily excited oscillation of frequency f_0 and subsequent interactions of the parametrically induced subharmonics $f_{1,2}$ with each other and/or with the primary wave. For example, in quadratic-nonlinear resonant systems with complex, non-equidistant mode

spectrum, favorable for the parametric decay of f_0 into slightly asymmetrical subharmonics ($f_0 = f_1 + f_2$, $f_{1,2} = f_0/2 \pm \Omega/2$, $\Omega \ll f_0$), the subsequent generation of the second harmonics $2f_{1,2}$ may result in appearance of the modulation spectral sidelobes near f_0 [7]. Alternatively, for strongly asymmetrical decay ($f_0 = f_1 + f_2$, $f_1 = \Omega \ll f_2$), the envelope self-modulation arises due to beatings between adjacent components f_0 and $f_2 = f_0 - \Omega$ [4].

In the present letter we report experimental observations and interpretation of MI phenomena in an acoustic resonator with an artificial crack-like defect. The effect is not reduced to any of the aforementioned MI types and is of a different, essentially dissipative origin, which can be common for waves of other physical nature as well. In acoustics, media containing contacts or crack-like defects (*e.g.*, rocks or damaged solids) constitute a wide class of materials exhibiting strongly nonlinear behaviour. Their microstructure-induced nonlinearity strongly differs from that related to weak anharmonicity of the interatomic potential. Along with conventional nonlinear elasticity, these materials may manifest both quasi-static [11, 12] and dynamic [13, 14] nonlinearity hysteresis and nonlinear thermoelastic absorption [15–17]. The acoustical MI reported here, exhibits a wealth of physically interesting features and is one of the phenomena related to peculiar nonlinear properties of micro-inhomogeneous materials.

The effect discussed, unlike previous observations [4, 7], did not imply multi-mode interactions and could be observed in the absence of subharmonics. Clear experimental evidence has been obtained that the effect is related purely to nonlinear dissipation, whereas eventual contributions of the elastic nonlinearity and wave velocity dispersion are not essential in contrast to [5, 6]. Important features of the MI are reproduced in the proposed instructive theoretical model, which generically has a certain resemblance, but does not reduce to equations describing the Van der Pol self-excited oscillator and its synchronization by an external sinusoidal signal [8]. The physical reason of the MI is the amplitude-dependent period-averaged self-transparency induced by the crack-like defect (although total losses still remain positive).

The resonators prepared were glass bars of 1 cm in diameter and about 20 cm in length

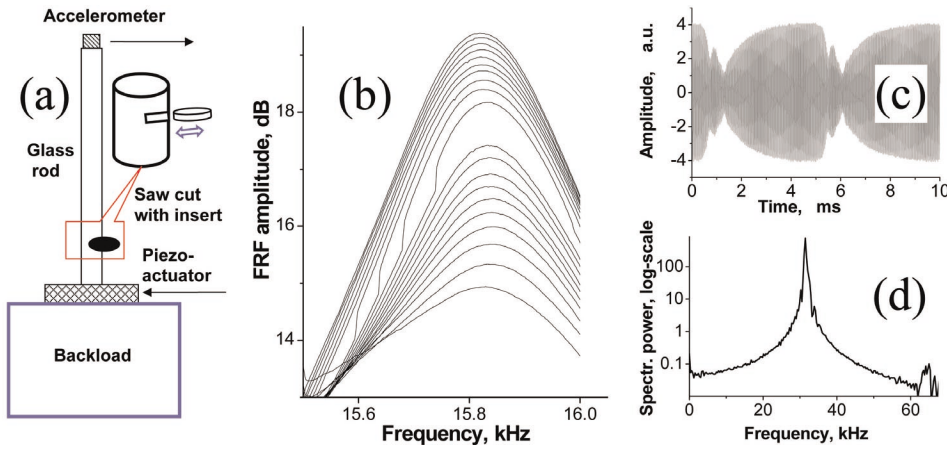

Fig. 1 – (a) Schematically shown experimental setup. (b) FRF for 2nd longitudinal (Young) eigenmode demonstrating induced transparency and exhibiting "jumps". Excitation amplitude increased in 0.5 dB steps. Without nonlinear dissipation (no insert in the saw cut) the curves practically coincided. (c) Example of temporal envelope waveform with well-developed self-modulation near resonator 4th mode, and (d) the respective spectrum of the signal demonstrating absence of the decay instability (subharmonics) accompanying the MI.

cemented onto a backload via a piezo-actuator (see fig. 1(a)). A light accelerometer at the free end of the bar provided the signal acquisition. About 1.5 cm from the backload a saw cut of 4 mm in depth and 1 mm thick was made. A small metal plate could be put in the saw cut in order to create an artificial crack-like defect. Preliminary measurements confirmed high linearity of the system without the inserted plate. With the plate inserted, as expected from the nature of the crack-like defect [15, 16], the acoustic response of the sample exhibits pronounced amplitude dependence. The latter is usually characterized by the resonance-frequency shift (due to the reactive part of the nonlinearity) and by the change in the quality factor (due to the dissipative part of the nonlinearity). At certain positions of the insert, the eigenmodes demonstrated a particularly interesting behavior in a rather wide (~ 10 dB) amplitude range: the resonance frequency remained almost unchanged while the quality factor increased strongly (up to 2-3 times). An example is shown in fig 1(b) presenting frequency response functions (FRF), that is the ratio of the accelerometer output to the excitation voltage for several driving amplitudes near the second eigenmode.

Two non-trivial effects in this amplitude range can be pointed out. The first one consists in abrupt vertical jumps in the FRF (visible in fig 1(a) at the flanks of the FRF curves) indicating a switching of the system from one regime to another. The second interesting effect is that the oscillations of the resonator under sinusoidal excitation can exhibit self-modulation. The observed waveforms and their spectral compositions (see an example in fig. 1(c), (d)) demonstrate that this self-modulation happens *without assistance of subharmonics, as well as without essential multi-mode interaction and in the absence of noticeable reactive nonlinearity.* These features indicate a MI mechanism different from those considered earlier [1–10] including those discussed previously in acoustics [4–7, 9]. The described setup allowed the study of the evolution of the self-modulation spectra as a function of the excitation amplitude and frequency, these dependencies appeared to be qualitatively very similar. For example, the 3D plot in fig. 2(a) presents a sequence of MI spectra exhibiting gradual variation of frequency for the main modulation sidelobes and formation of peculiar cross-like structures of an additional slower modulation, which depend on the driving amplitude.

The main observed MI features can be considered using an instructive 1D model of a resonator with sinusoidally driven boundary. The solution is searched as superposition of longitudinal eigenmodes. In the parameter range considered, the nonlinearity induced by the defect can be reasonably modeled as purely dissipative due to experimentally documented strong induced transparency and negligibly small nonlinear shift of the resonance frequencies. The defect is accounted in the equation via a delta-localized dissipation operator depending on the strain (or strain rate), which models the desired amplitude-dependent sound absorption. Using conventional procedures [8], for instantaneous amplitude $A(t)$ of any sinusoidally driven resonator mode near its eigenfrequency ω_0, an oscillator-type equation can be obtained:

$$\ddot{A} + 2\nu f(\dot{A})\dot{A} + \omega_0^2 A = F(t). \tag{1}$$

Here ν is the dissipation coefficient in the small-amplitude limit, when the normalized nonlinear-dissipation function $f(\dot{A})$ satisfies the condition $f(\dot{A} \to 0) \to 1$. The main controlling parameters ω_0 and ν (or quality factor $Q_0 = \omega_0/(2\nu)$) could be readily estimated from the shapes of the measured resonance peaks. The mode amplitude A is then searched in the form $A(t) = a(t)\cos(\omega t + \varphi(t))$, where $a(t)$ and $\varphi(t)$ are the slowly varying amplitude and phase of the oscillation driven by a sinusoidal force $F(t)$ at frequency ω and amplitude F_0. Substitution of this representation into (1) yields via harmonic balance [8] the following equations:

$$\begin{aligned} a\dot{\varphi} + a\Delta\bar{\omega} &= -\bar{F}_0\cos(\varphi), \\ \dot{a} + a\tilde{f}(a) &= -\bar{F}_0\sin(\varphi), \end{aligned} \tag{2}$$

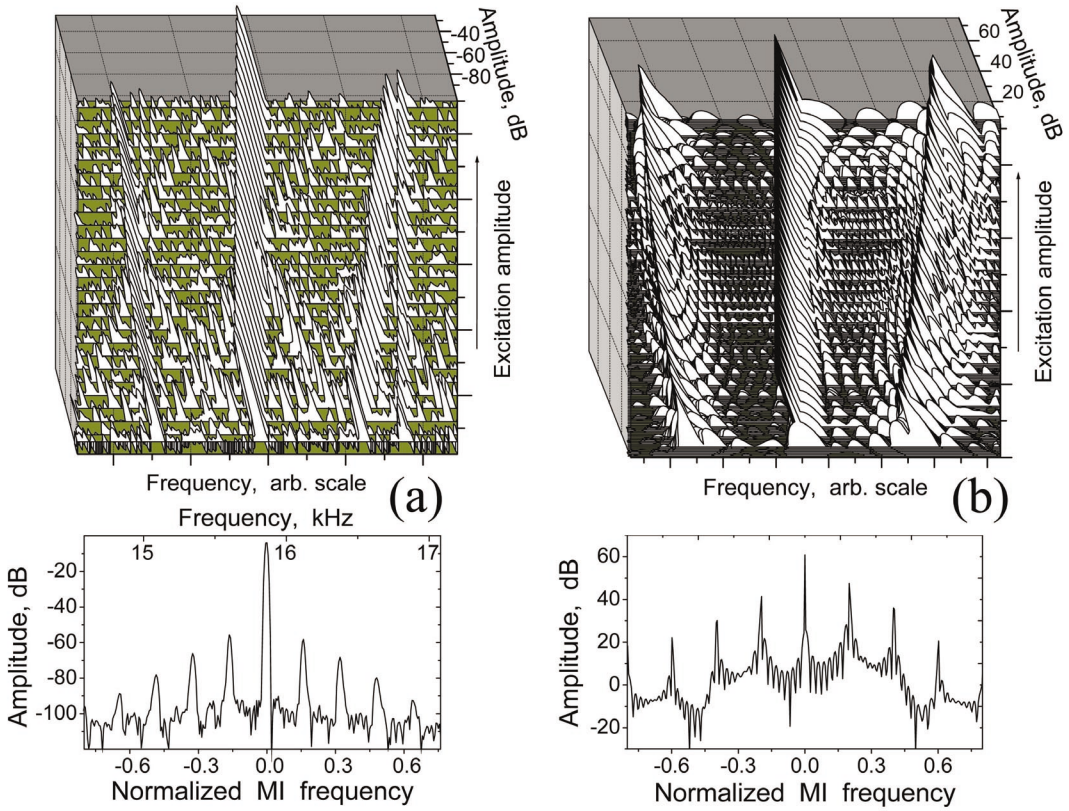

Fig. 2 – Evolution of the MI spectra *vs.* the driving amplitude and examples of a single spectrum. (a) Experimental data; (b) numerical simulations using eqs. (2), which exhibit normalized frequency scales of MI, $\bar{\Omega}$, and transitional cross-like structures for series of MI spectra similar to experiment.

where $\Delta\bar{\omega} = (\omega - \omega_0)/\Delta\omega_{1/2}$ is the normalized frequency detuning from the resonance, $\Delta\omega_{1/2} = \omega_0/(2Q_0)$ being its half-width. The time is also normalized $t \to \omega_0 t/(2Q_0) = \Delta\omega_{1/2} t$; $\bar{F}_0 = 2Q_0 F_0/(\omega\omega_0)$ is the normalized driving amplitude and the period averaged nonlinear dissipation function $\tilde{f}(a)$ depends only on even powers of a. For equilibrium points corresponding to $\dot{a} = 0$ and $\dot{\varphi} = 0$ system (2) yields the following equation:

$$a^2 \tilde{f}^2(a) = (\bar{F}_0^2 - \Delta\bar{\omega}^2 a^2). \tag{3}$$

The right-hand side of eq. (3) depends on driving conditions (amplitude and frequency) and, in the absence of reactive nonlinearity, $\partial(\Delta\bar{\omega})/\partial a = 0$, it represents a straight line in function of a^2 (below we denote it "loading line" L in fig. 3(a)). The left-hand side of eq. (3) describes the nonlinear dissipative properties, that will be more convenient for graphical analysis to characterize by the function $\Phi(a) = a\tilde{f}(a)$. This function exhibits a decreasing part $\Phi'(a) < 0$, if in a certain amplitude range the function $\tilde{f}(a)$ locally decreases faster than a^{-1}. Characteristic variants of stationary points, determined by intersection(s) between the loading line and dissipation function $\Phi(a)$ are shown schematically in fig. 3(a). Stability analysis of exponential perturbations $\propto \exp[\lambda t]$ for the linearized system (2) yields the characteristic values

$$\lambda_\pm = -[\Phi/a + \partial\Phi/\partial a \pm \sqrt{(\Phi/a - \partial\Phi/\partial a)^2 - 4(\Delta\bar{\omega})^2}]/2. \tag{4}$$

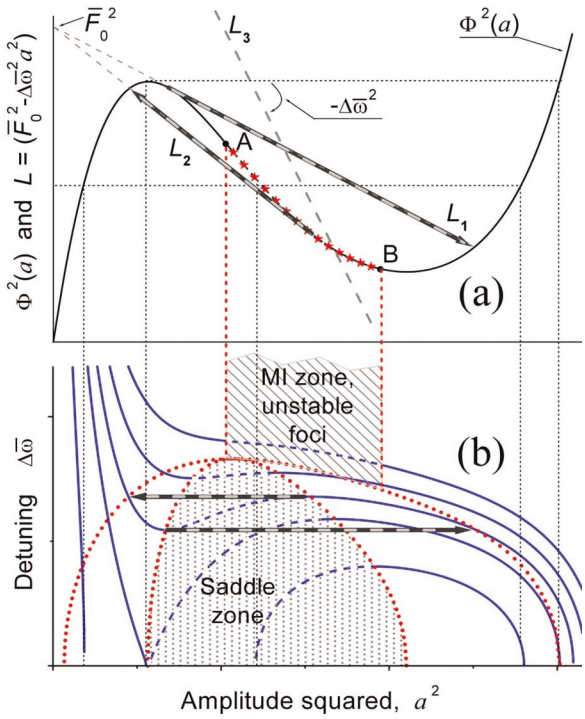

Fig. 3 – (a) Schematically shown left- and right-hand sides of eq. (3) illustrating different variants of equilibrium points. MI is possible within segment AB. (b) Corresponding structure of instability zones and resonance curve shapes (unlike fig. 1(a) the curves are not normalized to the excitation amplitude, and one-halves are shown with unstable parts indicated in dashed style). Dotted boundaries encounter zones of "jumps", the inner oval-type curve is for beginnings and the outer curve is for jump arrivals (see thick arrows in plots (a), (b)).

As is clear from fig. 3(a), at small $\Delta\bar{\omega}$, there are always one or two intersections with increasing parts of $\Phi(a)$. These intersections in accordance with (4) definitely correspond to stable equilibrium points that attract the system and prevent MI development (even in the presence of an intersection with the descending part of $\Phi(a)$). Only at sufficiently large $\Delta\bar{\omega}$ and $\bar{F}_0$, there may exist a single equilibrium point at the descending part of $\Phi(a)$ (see line L_3 in fig. 3(a)). However, according to eq. (4), even at the descending part the MI may develope only in region(s), where $\Phi(a)/a + \Phi'(a) < 0$, or equivalently $[a\Phi(a)]' = [\tilde{f}(a)a^2]' < 0$, which indicates a decrease of $\tilde{f}(a)$ faster than a^{-2}. In the energy terms, since $\tilde{f}(a)a^2$ is proportional to the energy dissipation rate (which is always positive in our system), condition $[\tilde{f}(a)a^2]' < 0$ corresponds to the locally negative differential energy dissipation.

The static equation (3) can be also considered as an implicit expression for the resonance curves with stable and unstable branches. In fig. 3(b) such a single-valued and several multi-valued curves are shown, for which the relation to the dissipation function plotted in fig. 3(a) is indicated by dashed lines. In the multi-valued zone of a resonance curve, there are normally three stationary amplitudes for given excitation parameters. The stability analysis (see eq. (4)) reveals that the two extreme equilibrium points are stable, while the intermediate third point is unstable (saddle-type). For multi-valued resonances, the equilibrium amplitude exhibits jumps at monotone variation either in excitation amplitude or frequency (for the latter case,

such jumps are indicated by arrows in both plots in fig. 3). The jumps begin at the intersection between the considered resonance curve and the inner filled-oval as indicated in fig. 3(b). Each point inside that oval is unstable and the border of the filled-oval is the boundary of a saddle-node bifurcation. The second oval-like region encounters the jump arrivals. Jumps between stable parts of the curves constituted of two separate branches may happen only at eventually strong enough perturbations. The MI zone, corresponding to single-equilibrium points located within segment AB in fig. 3(a), is indicated in fig. 3(b) by the dashed pattern.

At the threshold points A and B (fig. 3) defined by the condition $(\Phi(a)/a+\Phi'(a))|_{A,B}=0$, the imaginary part of $\lambda_\pm$ readily gives estimates of the normalized modulation frequency $\bar{\Omega}=\Omega/\Delta\omega_{1/2}$:

$$\bar{\Omega}_{A,B}=\sqrt{(\Delta\bar{\omega})^2-(\Phi'(a)|_{A,B})^2}. \tag{5}$$

At point A, the MI-threshold slope $(\Delta\bar{\omega})^2_{\min}$ of the loading line is equal to the slope $\Phi'(a)|_A$. Then eq. (5) yields the estimate $\bar{\Omega}_A\to 0$. In the right boundary point B (in which $\Phi'(a)|_B \ll \Phi'(a)|_A$, but the threshold slope remains roughly the same as in point A in fig. 3(a)), eq. (5) predicts that the near-threshold $\bar{\Omega}_B$ is of the order of the half-width $\Delta\omega_{1/2}$ of the resonance:

$$\bar{\Omega}_B\approx\sqrt{\Phi'|_A^2-\Phi'|_B^2}\approx\Phi'|_A=\tilde{f}(a)|_A\sim 1. \tag{6}$$

Experiments and direct numerical simulations based on eqs. (2) confirm prediction (6) of a rather fast and shallow near-threshold modulation around one threshold (B) and very slow and rather deep modulation in the vicinity of another threshold point A. The observed very similar evolution of MI as a function of the excitation frequency and amplitude is thus readily explained by the similar movement of the unstable equilibrium along segment AB due to variation of either $\Delta\bar{\omega}$ or $\bar{F}_0$ (see fig. 3(a)).

Note that occurrence of an additional reactive nonlinearity of the system should introduce amplitude dependence for the frequency detuning in the right-hand side of eq. (3), $\Delta\bar{\omega}=\Delta\bar{\omega}(a)$ (actually a slight shift of the resonance peak is visible in fig. 1). In such a case, the straight "loading lines" should become curved. However, qualitatively this curvature does not change the considered classification of the equilibrium points and does not cancel the conclusion on the crucial importance of the induced transparency for the existence of MI, although the MI-threshold values for $\bar{F}_0$ and $\Delta\bar{\omega}$ may be somewhat affected. Note further, that eventual "steps" on the dissipation function (*e.g.* due to threshold activation of additional contacts in the defect), may locally break within some part(s) of segment AB the differential negative dissipation condition $[a\Phi(a)]'<0$ necessary for MI develoment. However, this local stability should manifest itself only for very special initial conditions sufficiently close to the equilibrium. Numerical simulations confirm these conclusions and indicate that "globally" instability of segment AB persists. Besides, for gradually varying $\bar{F}_0$ or $\Delta\bar{\omega}$, the intersection of the loading line with the locally stable "step" may induce some transitional processes, which in addition to the main relatively fast modulation cause the appearance of a co-existing slow self-modulation. This additional modulation may disappear/reappear under monotonous variation of either frequency or amplitude of the excitation. Both the experimental observations and numerically simulated examples of a similar behavior are shown in fig. 2. For simulation in eqs. (2) we used the dissipation function of the form $\tilde{f}(a)=1-(3/4)a^2+(2.7/16)a^4$ with a "step" inducing local near-neutral stability $[a\Phi(a)]'\approx 0$ at $a=1.22\pm 0.01$ (threshold point A in fig. 3 was scaled to $a=1$).

Detailed discussion of the physical origin of the amplitude-dependent dissipation induced by the crack-like defect is beyond the scope of the present letter. One of the possible mechanisms (of a thermo-elastic type) was discussed in [15–17]: the acoustic transparency might be

caused either by the wave-induced modification of energy dissipation at individual contacts or by the disappearance of some of the sound absorbing contacts in the acoustic field of increasing amplitude. Also at the same type of defects, similar effects could arise due to friction or adhesion-type hysteresis (other hysteretic mechanisms may be relevant for waves of different nature). Indeed, the complete saturation of hysteresis at higher amplitudes, may provide the dissipation decrease as fast as a^{-2} (because the energy dissipation is saturated, whereas the accumulated elastic energy in the material continues to increase as a^2). Thus the considered MI mechanism can operate for oscillations and waves of another nature, which also exhibit sufficiently strong decrease in absorbtion with increase in amplitude (*e.g.* due to hysteresis saturation); this dissipative nonlinearity may or may not be accompanied by reactive nonlinearity. Returning to the discussed acoustic case we may underscore that the experimental setup with the artificial crack allowed us to realize the self-induced transparency in especially clear form, practically without complementary elastic nonlinearity. It is worthy to note that samples with natural cracks may also exhibit quite pronounced induced transparency [16]. However, real cracks are weakly controllable and reproducible, whereas the insert in the saw cut used in the described expriments provided a much easier way to imitate and reproduce different properties of cracks by slightly changing the insert position.

Artificial cracks similar to the one in the described experiments were succesfully used for imitation of real cracks in studies related to diagnostic applications of nonlinear effects [18]. Note finally that MI phenomena qualitatively similar to those discussed above were also observed for samples with real cracks [7].

* * *

The study was supported by the French-Russian program PECO-NEI-19118 and RFBR (grants 05-02-17355 and 06-02-72550).

REFERENCES

[1] Cross M. C. and Hohenberg P. C., *Rev. Mod. Phys.*, **65** (1993) 851.
[2] Van Tartwijk G. H. M. and Agrawal G. P., *Progr. Quantum Electron.*, **22** (1998) 43.
[3] Whitham G. B., *Linear and Nonlinear Waves* (Wiley, New York) 1974.
[4] Soustova I. A. and Sutin A. M., *Sov. Phys. Acoust.*, **21** (1975) 582.
[5] Planat M. and Hommady M., *Appl. Phys. Lett.*, **55** (1989) 103.
[6] Kivshar Yu. and Syrkin E., *Phys Lett. A*, **153** (1991) 125.
[7] Solodov I., Wackerl J., Pfeiderer K. and Busse G., *Appl. Phys. Lett.*, **84** (2004) 5386.
[8] Rabinovich M. I. and Trubetskov D. I., *Oscillations and Waves in Linear and Nonlinear Systems* (Kluwer, Dordrecht) 1989.
[9] Gusev V., *Wave Motion*, **33** (2001) 145.
[10] Streppel U., Michaelis D., Kowarschik R. and Bräuer A., *Phys. Rev. Lett.*, **95** (2005) 073901.
[11] Holcomb D., *J. Geophys. Res.*, **86** (1981) 6235.
[12] Tutuncu A., Podio A., Gregory A. and Sharma M., *Geophysics*, **63** (1998) 184.
[13] Solodov I. Yu. and Korshak B. A., *Phys. Rev. Lett.*, **88** (2001) 014303.
[14] Moussatov A., Castagnède B. and Gusev V., *Phys. Lett. A*, **301** (2002) 281.
[15] Zaitsev V., Gusev V. and Castagnède B., *Phys. Rev. Lett.*, **89** (2002) 105502.
[16] Zaitsev V., Gusev V. and Castagnède B., *Phys. Rev. Lett.*, **90** (2003) 075501.
[17] Fillinger L., Zaitsev V., Gusev V. and Castagnède B., *Acust.-Acta Acust.*, **92** (2006) 24.
[18] Ekimov A., Didenkulov I. and Kazakov V., *J. Acoust. Soc. Am.*, **106**, Pt. 1 (1999) 1289.